A Mutational Analysis of the Acetylcholine Receptor Channel Transmitter Binding Site

Gustav Akk, Ming Zhou, and Anthony Auerbach*
Department of Physiology and Biophysics, State University of New York at Buffalo, Buffalo, New York 14214 USA

ABSTRACT Mutagenesis and single-channel kinetic analysis were used to investigate the roles of four acetylcholine receptor channel (AChR) residues that are candidates for interacting directly with the agonist. The EC_{50} of the ACh dose-response curve was increased following α-subunit mutations Y93F and Y198F and ϵ-subunit mutations D175N and E184Q. Single-channel kinetic modeling indicates that the increase was caused mainly by a reduced gating equilibrium constant (Θ) in αY198F and ϵD175N, by an increase in the equilibrium dissociation constant for ACh (K_D) and a reduction in Θ in αY93F, and only by a reduction in K_D in ϵE184Q. This mutation altered the affinity of only one of the two binding sites and was the only mutation that reduced competition by extracellular K^+. Additional mutations of ϵE184 showed that K^+ competition was unaltered in ϵE184D and was virtually eliminated in ϵE184K, but that neither of these mutations altered the intrinsic affinity for ACh. Thus there is an apparent electrostatic interaction between the ϵE184 side chain and K^+ ($\sim 1.7 k_B T$), but not ACh^+. The results are discussed in terms of multisite and induced-fit models of ligand binding to the AChR.

INTRODUCTION

Nicotinic acetylcholine receptors (AChRs) are ion channels that are activated by cationic ligands such as acetylcholine (ACh) and tetramethylammonium (TMA). In adult muscle AChRs are pentamers with the subunit composition $\alpha_2\beta\delta\epsilon$, and each α-subunit houses, in part, an agonist binding site located ~30 Å above the membrane surface (Unwin, 1993; Valenzuela et al., 1994).

Electron crystallographic images of *Torpedo* AChRs suggest that each putative binding site is surrounded by three helical segments that twist when the channel opens (Unwin, 1995). Affinity labeling and functional studies also suggest that three regions of the α-subunit (residues 86–93, 148–153, and 190–198) participate in agonist binding (Devillers-Thiery et al., 1993). Certain aromatic amino acids (W86, Y93, W149, Y151, Y190, and Y198) and cysteines (C192 and C193) are labeled by the site-directed ligands DDF (Dennis et al., 1988; Galzi et al., 1990), nicotine (Middleton and Cohen, 1991), or lophotoxin (Abramson et al., 1989). Mutations of α-subunit tyrosines at positions 93, 90, and 198 reduce the affinity of the AChR for agonists (O'Leary and White, 1992; Tomaselli et al., 1991; Sine et al., 1994; Nowak et al., 1995; Chen et al., 1995), whereas a G-to-S mutation of α-subunit residue 153 slows the agonist dissociation rate constant and causes a slow channel congenital myasthenic syndrome (Sine et al., 1995).

There is substantial evidence that the binding pockets are not confined to the α-subunits. In *Torpedo*, the two sites have distinct affinities for D-tubocurarine, a competitive antagonist of nicotinic receptors (Sine and Taylor, 1980). This ligand labels both the γ- and δ-subunits (Pedersen and Cohen, 1990). Further evidence of non-α-subunit participation in agonist binding comes from cross-linking studies that reveal two acidic residues in the δ-subunit (D180 and E189) that alter the apparent affinity for ACh and have been proposed to interact directly with the quaternary amine moiety of ACh (Czajkowski and Karlin, 1991; Czajkowski et al., 1993). There is similar evidence that negatively charged residues in the γ-subunit interact electrostatically with the agonist molecule (Martin et al., 1996).

These studies suggest the transmitter binding sites are generated by residues in the α and the adjacent subunits (Blount and Merlie, 1989; Pedersen and Cohen, 1990; Sine and Claudio, 1991; Prince and Sine, 1996; Tsigelny et al., 1997; for a review see Karlin and Akabas, 1995). This view is supported by electron microscopic images that reveal significant structural differences between the two binding sites of the *Torpedo* AChR (Unwin, 1996). However, functional studies of $\alpha_2\beta\delta\epsilon$ mouse AChR show that the equilibrium dissociation constant for small agonists such as ACh are similar at the two binding sites (Akk and Auerbach, 1996; Wang et al., 1997; Salamone et al., manuscript submitted for publication); thus the relative influences of short-range versus long-range interactions between non-α residues and the ligand at its docking site remain to be determined.

The binding of transmitter is not a simple diffusional process because the association rate constant for TMA is >10 times slower than for larger molecules such as ACh and carbamylcholine (Zhang et al., 1995). In $GABA_A$ receptor channels, smaller agonists also associate more slowly than larger agonists (Jones et al., 1998). One explanation for this behavior is that the binding pathway is an extended structure (Unwin, 1993) and that an agonist experiences energy barriers and wells along its trajectory from the bulk solution to the ligand docking site. Alternatively, an agonist-dependent conformational change in the protein may be

Received for publication 20 February 1998 and in final form 17 September 1998.

Address reprint requests to Dr. Anthony Auerbach, Department of Biophysical Sciences, SUNY-Buffalo, 118 Cary Hall, Buffalo, NY 14214. Tel.: 716-829-2435; Fax: 716-829-2415; E-mail: auerbach@buffalo.edu.

0006-3495/99/01/207/12 $2.00

required to stabilize the ligand at the docking site, and the rate constants for this "induced fit," rather than diffusion, determine the apparent association rate constant.

Another salient feature of agonist association in AChR is that inorganic cations such as Na^+ and K^+ compete with ACh for access to the agonist binding site (Akk and Auerbach, 1996). Because of this competition, in 150 mM NaCl the apparent ACh association rate constant is about half its value in pure water. This raises the possibility that mutations that alter the apparent affinity of the AChR do so by interfering with ion competition, rather than by altering ligand-protein interactions per se.

We have used site-directed mutagenesis and single-channel kinetic analysis to investigate the roles of four residues (αY93, αY198, ϵD175, and ϵE184), all of which are candidates for interacting directly with the bound agonist based on affinity labeling and functional studies. We have dissected the effect of the mutations on single-channel dose-response profiles into more fundamental components: equilibrium and rate constants for AChR activation, and the equilibrium inhibition constant and selectivity for monovalent cations. The results suggest that only one of these residues, ϵE184, determines the equilibrium dissociation constant of inorganic cations (but not ACh) via a direct electrostatic interaction. The results are discussed in terms of different physical models for the binding of ligands to the AChR transmitter binding site.

MATERIALS AND METHODS

Mouse AChR subunit cDNA (α, β, δ, ϵ) was provided by Dr. Steve Sine, who obtained the clones (originally from Dr. J. Merlie) from Drs. H. Lester and N. Davidson. The genes were subcloned into CMV-based expression vectors pRBG4 (Sine, 1993) or pcDNAIII (Invitrogen, San Diego, CA). Mutant clones αY93W and αY198F were provided by Dr. Sine. The remaining mutants (ϵD175N, ϵE181Q, ϵE184Q, ϵE184K, ϵE184D) were created using overlap polymerase chain reaction (Higuchi, 1990). The "wild-type" α-subunit had a mutation in the M4 segment, αV433A. This mutation has essentially no effect on the activation rate constants (Salamone et al., manuscript submitted for publication).

Human embryonic kidney (HEK) 293 cells were transiently transfected by calcium phosphate precipitation (Ausubel et al., 1992). A total of 3.6 μg DNA/35-mm culture dish in the ratio 2:1:1:1 (α:β:δ:ϵ) was used. The medium was changed 24 h after transfection, and electrophysiological recordings were started 48 h later.

Because some of the mutants we examined were in the ϵ-subunit, we also examined the properties of channel formed when only the α-, β-, and δ-subunits were expressed (Charnet et al., 1992). The expression levels of such "ϵ-less" AChR were low, but in some cases single-channel currents with the conductance properties of $\alpha_2\beta\delta\epsilon$ AChR could be recorded. These channels had very long open channel lifetimes and on this basis were readily distinguishable from the ϵ-mutant AChR we examined. We conclude that all of the results presented in this study concern AChR having the full complement of subunits.

Electrophysiological recordings were performed using the patch-clamp technique in the cell-attached configuration (Hamill et al., 1981). The bath solution was Dulbecco's phosphate-buffered saline (in mM): 137 NaCl, 0.9 $CaCl_2$, 2.7 KC, 1.5 KH_2PO_4, 0.5 $MgCl_2$, 6.6 Na_2HPO_4 (pH 7.3). The pipette solution contained (in mM) 142 KCl, 1.8 $CaCl_2$, 1.7 $MgCl_2$, 5.4 NaCl, 10 HEPES (pH 7.4). In experiments at low ionic strength, only the concentration of KCl was varied. The interior of the pipette was held at +70 mV; assuming a reversal potential of 0 mV and a conductance of 70 pS, we estimate that the membrane potential was typically −100 mV. The temperature was 22°C.

Details of the recording and analysis are described by Akk et al. (1996). Briefly, clusters were elicited by using high concentrations of ACh (Sakmann et al., 1980). Open and closed intervals within clusters were detected using a half-amplitude threshold crossing criterion (Sachs, 1983). Histograms of closed and open interval durations were fitted by sums of exponentials. Usually the predominant component of the closed interval duration histogram represented the slowest intracluster component. Clusters were defined as groups of openings separated by gaps that were shorter than a critical duration. This duration was at least four times longer than the time constant of the predominant component of intracluster closed intervals and was never shorter than 5 ms. Clusters less than 100 ms in duration were rejected from further analysis. The closed interval durations of intracluster gaps were compiled and fitted by sums of exponentials to check the validity of the cluster definition criterion. The inverse of the predominant component of the open and closed intracluster closed interval distribution was defined as the effective closing rate (α') and opening rate (β'), respectively. Clusters were extracted from the original data file for further processing.

The extracted clusters were idealized using the segmental k-means algorithm (Qin et al., 1996a; program SKM) to obtain a list of idealized currents. The analysis bandwidth was typically 10 kHz. To determine the rate constants, interval durations were fitted (using a maximum likelihood procedure) by their corresponding probability density functions, assuming a Markov kinetic scheme (Qin et al., 1996; program MIL). The algorithm used a first-order correction for missed events; the dead time was 20 μs. One scheme that was used to encode AChR activation was

$$C \underset{k_{-1}}{\overset{Ak_{+1}}{\rightleftharpoons}} AC \underset{k_{-2}}{\overset{Ak_{+2}}{\rightleftharpoons}} A_2C \underset{\alpha}{\overset{\beta}{\rightleftharpoons}} A_2O \qquad \text{Model 1}$$

where A is the agonist concentration, k_{+1} and k_{+2} are the agonist association rate constants, k_{-1} and k_{-2} are the agonist dissociation rate constants, β is the channel opening rate constant, and α is the channel closing rate constant. In model 1, when the binding sites are equivalent, $k_{+1} = 2k_{+2}$ and $k_{-2} = 2k_{-1}$, and there are only four free parameters. In this case the probability of being open within the cluster (P_o) is described by an equilibrium dissociation constant ($K_D = k_-/k_+$) and a gating equilibrium constant ($\Theta = \beta/\alpha$). During the kinetic modeling, β was constrained to be the maximum value of β'.

RESULTS

Single-channel currents and dose-response curves

Fig. 1 shows example clusters and interval duration histograms from wild-type and mutant AChR. In all of the mutants, the open-channel lifetimes are shorter and the closed-channel lifetimes are longer (at a given ACh concentration) than the wild type.

Dose-response curves are shown in Fig. 2, and the parameters are given in Table 1. For all mutants, the EC_{50} of the P_o versus concentration curve was larger than the wild type. For ϵD175N and αY93W the maximum P_o was significantly lower than the wild type. To determine the extent to which the P_o curves were influenced by changes in cluster open and closed lifetimes, these parameters are plotted as a function of the ACh concentration in Fig. 2, *B* and *C*. The open-channel lifetime did not change with concentration and was within a factor of 4 for all AChRs that were examined. Thus the changes in the P_o profiles arise mainly from changes in rate constants that influence closed durations.

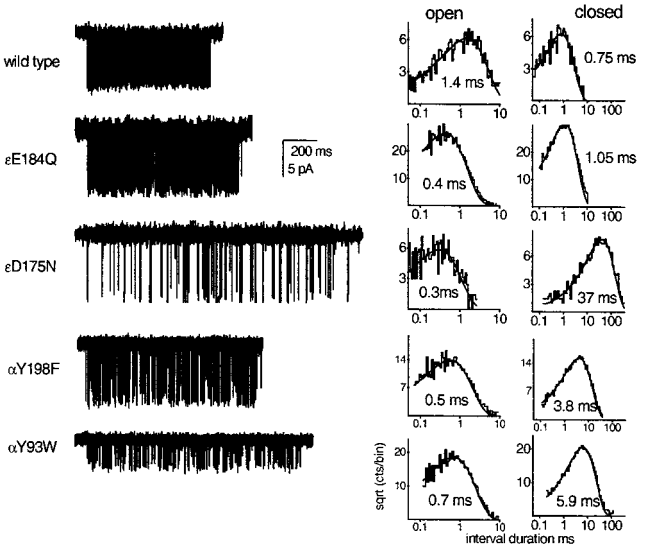

FIGURE 1 Single-channel current clusters from adult-type AChR. Open and closed interval duration histograms are shown to the right. The [ACh] was 50 μM, except for αY93W, which was 2 mM ACh (membrane potential = −100 mV, 22°C). The open intervals are shorter and the closed interval are longer in the mutant AChR. The lower amplitude of the αY93W currents is caused by channel block by ACh.

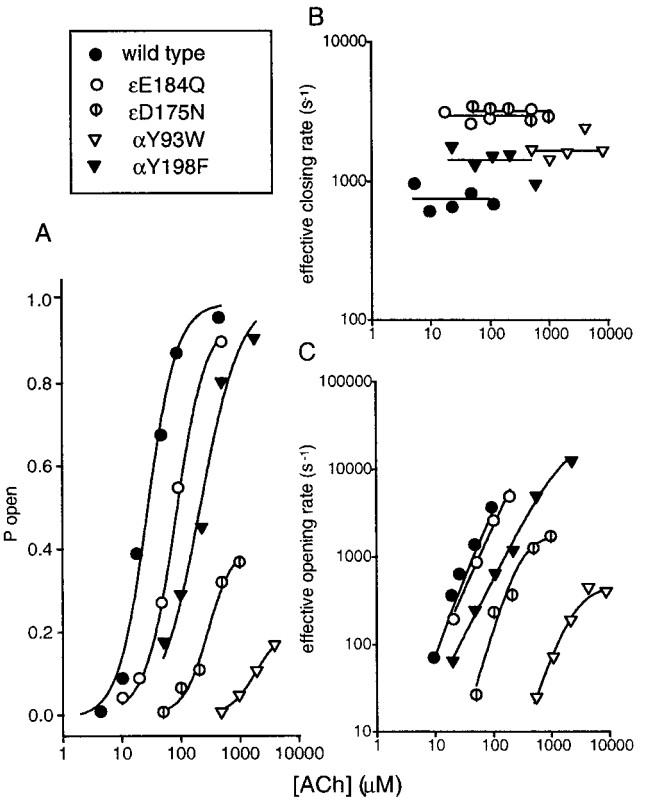

FIGURE 2 Dose-response curves. (*A*) The probability of being open within a cluster (P_{open}). (*B*) The effective closing rate (α') is not dependent on the [ACh]. (*C*) The effective opening rate (β'). The P_o and β' curves for the mutant AChR are shifted to the right compared to the wild type. The solid line is fit by Hill equation (see Table 1). Each symbol is one patch.

The effective opening rate (β') is a complex function that depends on all of the rate constants of model 1 except α and that approaches β at high agonist concentrations. Fig. 2 *C* shows that the EC_{50} of this parameter varied ~100-fold between wild-type and mutant AChRs, and that β was substantially smaller in ϵD175N and αY93W than in the wild type. The results of fitting the β' curves are given in Table 1. Compared to the wild type, there was no detectable change in β in ϵE184Q, an approximately threefold reduction in αY198F, a ~33-fold reduction in ϵD175N, and a ~130-fold reduction in αY93W.

Because we could not measure a saturation in β' for ϵE184Q, we quantified the limiting value of β' by using an agonist that supports a slower opening rate constant, TMA, and a mutant AChR, αG153S. This mutation does not substantially alter the channel opening rate constant but facilitates the measurement of β, because agonist dissociation is slowed, and the lifetime and number of sojourns in the A_2C state are increased (Sine et al., 1995). In αG153S + ϵE184Q AChR activated by TMA, we estimate $\beta = 7374 \pm 2069$ s^{-1} (mean ± SD; three patches), which is similar to the value of β for wild-type AChRs activated by TMA (8150 s^{-1}; Akk and Auerbach, 1996). If we assume that the effects of both mutations are independent of the nature of the agonist, then this result suggests that the ϵE184Q mutation does not significantly alter the channel opening rate constant when ACh is the agonist.

Kinetic modeling: equal binding sites

Rate constants governing receptor activation were determined by fitting the parameters of model 1 (i.e., assuming equivalent transmitter binding sites) to a list of idealized intracluster interval durations. β was constrained to be the value obtained from fitting the β' curve (Table 1), or in the case of ϵE184Q, 60,000 s^{-1}. The results are shown in Table 2.

αY93W causes an almost 100-fold decrease in k_+. This, along with a 10-fold decrease in k_-, is the basis for the ~10-fold higher K_D for ACh in this mutant. However, the largest consequence of the Y-to-W mutation is a 130-fold decrease in β. In contrast, α was essentially unchanged. Together, these rather dramatic effects on channel opening and ligand binding result in a ~70-fold shift in the EC_{50} of the P_{open} dose-response curve (Fig. 2 *A*).

The Y198F mutation in the α-subunit has a much more modest effect on AChR activation. Both k_+ and k_- are reduced approximately twofold, with little net effect on K_D. However, the mutation both reduces β and modestly increases α, thereby lowering the gating equilibrium constant ~10-fold. Although the α198 site has been proposed by others (O'Leary and White, 1992; Sine et al., 1994) to interact directly with ACh in the binding pocket, these results indicate that the Y-to-F mutation mainly alters gating, and not binding, and is therefore not a good candidate for making direct contact with agonist.

TABLE 1 Dose-response parameters of wild-type and mutant receptors

Receptor	$P_{o,max}$	EC_{50} (μM)	n_H	β (s^{-1})	EC_{50} (μM)	n_H	n
Wild type	0.96 ± 0.04	28 ± 3	1.8 ± 0.3	60,000*	532 ± 79	1.6 ± 0.1	6
αY93W	0.21 ± 0.01	1911 ± 103	1.9 ± 0.2	463 ± 112	2532 ± 805	1.9 ± 0.3	4
αY198F	1.0 ± 0.1	219 ± 53	1.3 ± 0.3	23400 ± 8928	1754 ± 846	1.3 ± 0.1	5
ϵD175N	0.41 ± 0.1	289 ± 59	2.1 ± 0.6	1775 ± 805	302 ± 156	2.2 ± 0.6	5
ϵE184Q	0.86 ± 0.1	82 ± 17	1.9 ± 0.7	60,000*	785 ± 161	1.5 ± 0.1	5
ϵE184K	0.67 ± 0.03	80 ± 7	1.7 ± 0.2	7762 ± 1364	190 ± 52	1.5 ± 0.1	7
ϵE184D	0.45 ± 0.03	125 ± 22	2.5 ± 1.0	4128 ± 1260	214 ± 126	1.6 ± 0.6	6
ϵE184I	0.44 ± 0.03	119 ± 29	2.0 ± 0.8	4991 ± 635	217 ± 68	1.5 ± 0.3	5
ϵE184A	0.95 ± 0.01	43 ± 2	1.8 ± 0.3	60,000*	514 ± 84	1.5 ± 0.1	5

Dose-response parameters for AChRs activated by ACh (142 mM KCl, −100 mV, 22°C). The probability of being open within a cluster (P_o) and the effective opening rate (β') versus [ACh] profiles were fitted by the Hill equation, $x = m/(1 + (EC_{50}/[ACh]^{nH})$, where x is the response (P_o or β'), n_H is the Hill coefficient, and m is the maximum response ($P_{o,max}$ or β). The fitted curves are shown in Figs. 2 and 6. Values are ± SD.
* Not obtained by fitting the β' dose-response curve (β in ϵE184Q, and A were assumed to be the same as in the wild type).

ϵD175 is homologous to residues in the γ- and δ-subunits that have been proposed to interact directly with the positively charged nitrogen of ACh (Czajkowski et al., 1993). Kinetic modeling indicates that the mutation ϵD175N significantly reduces both k_+ and k_-, with essentially no change in K_D. This mutation also has a large effect on gating, with a >30-fold decrease in β and an approximately twofold increase in α. The relatively minor effect on the K_D consequent to the loss of charge at this position does not support the hypothesis that this residue stabilizes the bound ACh ligand via a direct electrostatic interaction. Rather, the kinetic results suggest that this mutation decreases the mobility of ACh between the bulk solution and the transmitter docking site.

The ϵE184Q mutation was also modeled assuming equivalent transmitter binding sites and a channel opening rate constant of 60,000 s^{-1}. The rate constant estimates (Table 2) indicate that the mutation modestly increases k_+ and α and substantially increases k_-, with the combined effect of these alterations being a fourfold increase in the EC_{50} of the P_o profile.

Kinetic modeling: unequal binding sites

If the transmitter binding sites are generated by α-ϵ and α-δ subunit pairs, then an ϵ-subunit mutation might be expected to alter ACh association and dissociation at only one of the two sites. To test this possibility, ϵE184Q currents from four patches (50 μM ACh, −70 mV, 62,228 intervals) were fitted using kinetic schemes that allow for unequal binding. The results are shown in Fig. 3. Note that in these experiments the membrane potential was 30 mV more depolarized than in the previous experiments and that this degree of depolarization increases the closing rate constant and reduces the gating equilibrium constant ~1.6-fold (Auerbach et al., 1996). As a basis for comparison, for these files the log likelihood (LL) of the fit by model 1 (i.e., assuming equal binding sites) and β = 60,000 s^{-1} was 389,647.

First, model 1 was used after removing the constraints of equal association and dissociation rate constants. We were unable to fit the intervals of ϵE184Q AChR using this scheme (which had five free parameters); the rate constants of the model would not converge. We hypothesize that this

TABLE 2 AChR activation rate constants

Receptor	k_+ (μM^{-1} s^{-1}) (in 142 mM KCl)	κ_+ (μM^{-1} s^{-1}) (in pure water)	k_- (s^{-1})	α (s^{-1})	Θ (β/α)	n
Wild type	111	259	18020 ± 422	1321 ± 15	45	4
αY93W	1.3	3.0	2010 ± 141	1312 ± 15	0.35	4
αY198F	44	97	9300	2459	4.5	4
ϵD175N	8.5	18	1580 ± 67	3141 ± 39	0.57	4
ϵE184Q	260	396	75000*	1906 ± 34	31	3
ϵE184K	107	109	6057 ± 308	3456 ± 39	2.2	4
ϵE184D	41	137	3762 ± 235	4935 ± 63	0.8	4
ϵE184I	—	—	—	1176 ± 21	4.0	5
ϵE184A	—	—	—	1539 ± 155	39	4

Rate constants for AChR activated by ACh (142 mM KCl, −100 mV, 22°C), obtained by fitting model 1 (assuming equivalent binding sites) to intracluster open and closed interval durations. k_+ is the association rate constant in 142 mM KCl, κ_+ is the association rate constant in pure water computed from k_+ and the equilibrium inhibition constant for K^+ (see Fig. 7), k_- is the dissociation rate constant, α is the closing rate constant (estimate from single-channel modeling, except for ϵE184I and ϵE184A, which are the inverse of the mean open channel lifetime), and Θ is the ratio of the opening rate constant (β; Table 1) and α. Values are ±SD. n is the number of patches.
* The rate constant was fixed during the optimization.

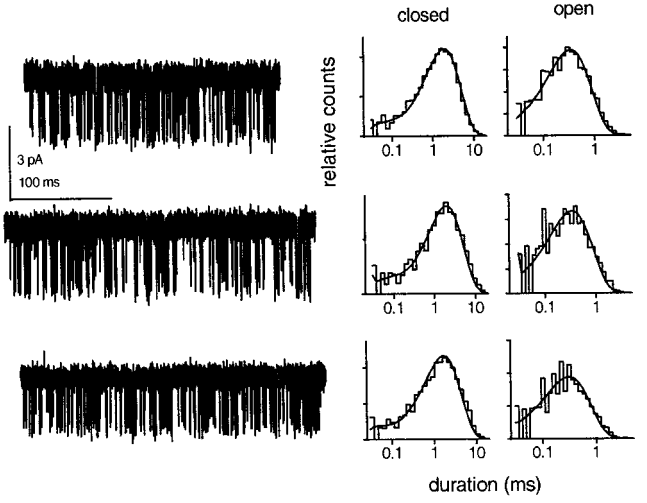

FIGURE 3 Kinetic analysis of ϵE184Q AChRs. One cluster and the closed and open interval duration histograms are shown for three patches (50 μM ACh, −40 mV). The solid lines are drawn from the fitted rate constants (±SD) of model 2. Top (43 clusters, 27,435 events): k_{+1} = 117 ± 6 μM^{-1} s^{-1}, k_{-1} = 16,464 ± 3107 s^{-1}, β^* = 51 ± 7 s^{-1}, α^* = 3276 ± 32 s^{-1}. Middle (31 clusters, 8774 events): k_{+1} = 93 ± 8 μM^{-1} s^{-1}, k_{-1} = 13,730 ± 3236 s^{-1}, β^* = 50 ± 8 s^{-1}, α^* = 3248 ± 51 s^{-1}. *Bottom* (31 *clusters*, 8774 *events*): k_{+1} = 120 ± 12 μM^{-1} s^{-1}, k_{-1} = 26,831 ± 8766 s^{-1}, β^* = 84 ± 28 s^{-1}, α^* = 3694 ± 84 s^{-1}. The rate constants k_{+1} and k_{-1} are the same in both ϵE184Q and wild-type AChRs, suggesting that this mutation increases ACh dissociation (by about fivefold) only from one transmitter binding site.

was because in this mutant, sojourns in the A_2C state are both rare and brief and are largely undetected. As a consequence, there were only two closed interval components in the idealized record, and kinetic models with more than two closed states could not be fitted.

We approached the problem of estimating the association and dissociation rate constants for ϵE184Q in two ways. First, using model 1, we fixed β (60,000 s^{-1}) and k_{-2} (150,000 s^{-1}) and allowed k_{+1}, k_{-1}, and α to be free parameters. The results were (mean ± SD): k_{+1} = 128 ± 5 μM^{-1} s^{-1}, k_{-1} = 18,238 ± 2247 s^{-1}, k_{+2} = 183 ± 14 μM^{-1} s^{-1}, and α = 4784 ± 29 s^{-1}. Allowing the binding sites to have different rate constants greatly improved the fit for the same number of free parameters (LL = 389,751, or a log likelihood ratio of 104). This result suggests that in the ϵE184Q mutant the equilibrium dissociation constants at the two sites are significantly different. From the above rate constants we calculate an equilibrium dissociation constant for each site: K_a = 142 μM and K_b = 819 μM. From this analysis we conclude that the difference in affinity between the sites arises mainly from a 14-fold faster dissociation rate constant at one site, which is presumably the mutated α-ϵ site.

We used another approach that did not require constraining k_{-2} to a specific value. If the A_2C state is vanishingly brief, model 1 condenses to

$$C \underset{k_{-1}}{\overset{Ak_{+1}}{\rightleftharpoons}} AC \underset{\alpha^*}{\overset{A\beta^*}{\rightleftharpoons}} A_2O \qquad \text{Model 2}$$

where

$$\beta^* = \frac{Ak_{+2}}{1 + k_{-2}/\beta} \quad \text{and} \quad \alpha^* = \frac{\alpha}{1 + \beta/k_{-2}} \qquad (1)$$

When model 2 was used without constraints (four free parameters), the optimal rates (simultaneous fit to three patches) were k_{+1} = 104 ± 3 μM^{-1} s^{-1}, k_{-1} = 19,924 ± 2042 s^{-1}, β^* = 66 ± 6 s^{-1}, and α^* = 3534 ± 26 s^{-1} (LL = 389,754, or a log likelihood ratio of 107; the rate constants for the fit to each patch are given in the legend of Fig. 3). From these rate constants we estimate that K_a = 192 μM, which is similar to the wild type (160 μM). From Eq. 1, to estimate the remaining rate constants, we need to estimate the ratio β/k_{-2}. Although we have assumed that β = 60,000 s^{-1}, in this analysis we have no information regarding the value of k_{-2}, other than it is significantly greater than β.

Although the equilibrium dissociation constants of the two transmitter binding sites in wild-type AChRs are the same, the association and dissociation rate constants may be ~2.5 times faster at one site (Salamone et al., manuscript submitted for publication). At the slow site, the association rate constant is ~110 μM^{-1} s^{-1}, and the dissociation rate constant is ~17,000 s^{-1}. These values are similar to k_{+1} and k_{-1} of ϵE184Q AChR, which suggests that this ϵ-subunit mutation specifically alters the fast binding site. We therefore speculate that the properties of the slow binding site are determined by the α- and δ-subunits, and the properties of the fast binding site are determined by the α- and ϵ-subunits.

The effect of the ϵE184Q mutation at the fast site can be estimated if we assume that only the dissociation rate constant is affected. In wild-type AChR, k_+ at the fast site is ~300 μM^{-1} s^{-1} (Salamone et al., manuscript submitted for publication). If the ϵ-subunit mutation only changes the dissociation rate constant for this site, then from β^* and Eq. 1 we calculate that k_- at this site in ϵE184Q AChRs is ~3.5 times faster than the channel opening rate constant, i.e., it is ~210,000 s^{-1}.

From these considerations we hypothesize that the E-to-Q mutation in the ϵ-subunit has a single effect, to increase the dissociation rate constant approximately fivefold. As a consequence, we estimate that in ϵE184Q AChR the K_D of the α-δ site is ~160 μM, and the K_D of the α-ϵ site is ~800 μM. Note that the shape of the P_{open} dose-response curve is not sensitive to affinity differences of the binding sites, and a fivefold difference in the equilibrium dissociation constant would not cause a measurable deviation from the equal binding site curve.

Effect of the ionic environment

Na^+ and K^+ compete with ACh for the transmitter binding sites (Akk and Auerbach, 1996). As a consequence, the k_+ estimates are sensitive to the concentrations of these inorganic cations in the extracellular solution, as well as to

mutations that influence the equilibrium constant for inhibition (K_I) by these ions. We therefore set out to determine the effect of the binding site mutations on the K_I for the predominant extracellular cation, K^+.

This information is doubly useful. First, it indicates the extent to which the salient residue interacts with inorganic cations when they are bound to the receptor. Second, the K_I value can be used to correct the observed association rate constants measured in 142 mM KCl, thereby allowing a more accurate picture of the effect of the mutations with regard to the ACh affinity per se.

Fig. 4 shows the effect of varying the concentration of KCl in the patch pipette on k_+ for ACh, estimated by kinetic modeling (assuming equal binding sites). As the extracellular KCl concentration increases, k_+ decreases because K^+ and ACh compete for a site (or sites) in the binding pathway. The results were fitted by

$$k_+ = \frac{\kappa_+}{1 + \frac{[\mathrm{KCl}]}{K_I}} \quad (2)$$

where κ_+ is the association rate constant for ACh in pure water.

The fitted values of K_I for the wild-type and mutant AChRs are shown in Table 3. Of the four positions that were examined, only the ϵE184Q mutation had a significant effect on the K_I for K^+, which increased by approximately threefold. This result suggests that the ϵE184 residue interacts favorably with the inorganic cation binding site(s), whereas the ϵD175, αY93, and αY198 residues do not.

In wild-type AChRs, the K_I for Cs^+ is about three times lower than that of K^+ (Akk and Auerbach, 1996). We next examined whether the ϵE184Q mutation altered the ion selectivity of the inorganic cation binding site. Fig. 5 shows dose-response curves for both wild-type and ϵE184Q AChR in the presence of Na^+, K^+, and Cs^+. In wild-type AChR,

TABLE 3 Equilibrium constants for K^+ inhibition and ACh dissociation

Receptor	K_I for K^+ (mM)	K_D for ACh (μM) (in 142 mM KCl)	κ_D for ACh (μM) (in pure water)
Wild type	92	162	70
αY93W	109	1546	649
αY198F	79	211	75
ϵD175N	157	186	98
ϵE184Q	486	1011	783
ϵE184K	1600	69	64
ϵE184D	88	151	58
ϵE184I	—	114	88*
ϵE184A	—	416	320*

K_I is the equilibrium inhibition constant for K^+, K_D is the equilibrium dissociation constant for ACh^+ in 142 mM KCl, and κ_D is the equilibrium dissociation constant for ACh^+ in pure water. The values for wild type, αY93W, αY198F, and ϵD175N were estimated assuming equivalent binding sites (Eq. 2, Fig. 3); the values for the ϵE184 mutants were computed assuming distinct affinities for ACh (Eq. 4) and K^+ (Eqs. 8 and 9) at the two sites (see Fig. 8) and pertain only to the α-ϵ transmitter binding site. * Calculated assuming that these mutations had the same effect on K_I as ϵE184Q, i.e., K_I = 486 mM.

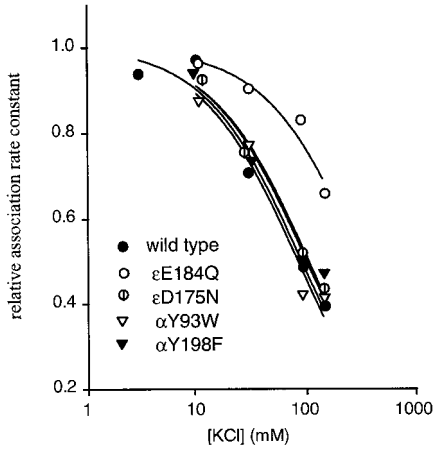

FIGURE 4 The ACh association rate constant versus the extracellular concentration of KCl. The association rate constant was estimated by single-channel kinetic analysis and was normalized to the extrapolated value in pure water. Each symbol is the mean of one to five patches. As the [KCl] increases, the ACh association rate decreases because of increased competition. The [KCl] that reduces the ACh association rate constant by half is the equilibrium inhibition constant for K^+ (K_I) (see Table 3).

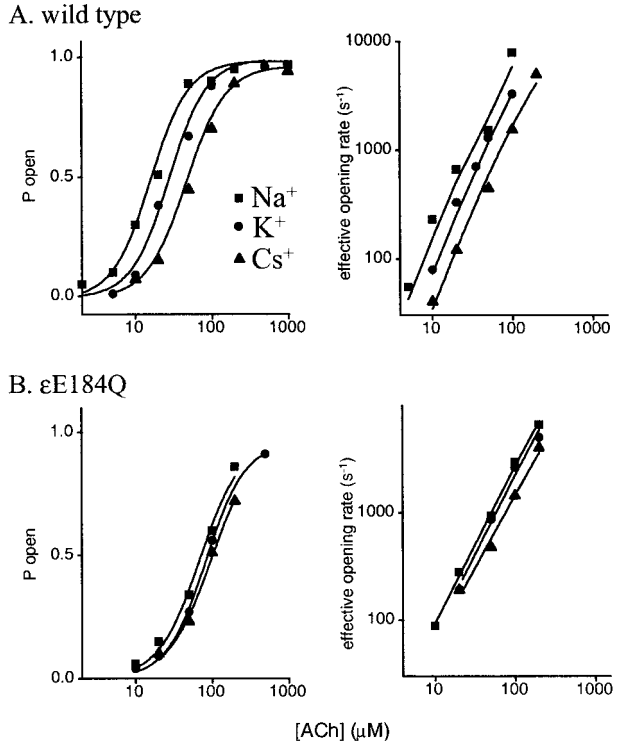

FIGURE 5 Dose-response curves for wild-type and ϵE184Q AChRs in different ionic environments. (*A*) P_o versus [ACh] for wild-type receptors. The EC_{50} depends on the nature of the extracellular cation in the sequence $Na^+ < K^+ < Cs^+$. This shift is due to different K_I's for each ion. (*B*) β' versus [ACh] curve for wild-type AChR. (*C*) P_{open} versus [ACh] for ϵE184Q receptors. The shift in EC_{50} is decreased, indicating that the mutation has reduced the selectivity between inorganic cations. Each symbol is one patch.

the increased EC_{50} values in the presence of these ions is caused by a reduction in k_+ caused by increased ion competition (Eq. 2). Fig. 5 *C* shows that the dose-response curve of the ϵE184Q mutant AChR is substantially less affected by changes in the ionic composition of the extracellular solution. We conclude that the ϵE184Q mutation reduces the discrimination between inorganic cations, which is consistent with the proposal that this residue interacts with an inorganic cation-binding site.

Estimating distinct equilibrium dissociation constants

If the two binding sites (a and b) are independent but have different equilibrium dissociation constants (K_a and K_b), then the following kinetic scheme is appropriate for quantitative analysis:

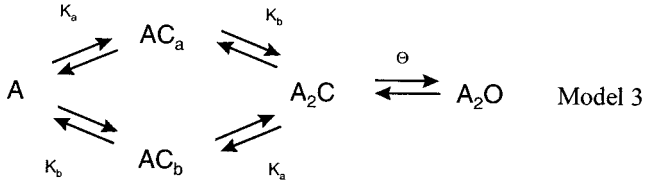

where AC_a is a receptor with only site a occupied, and AC_b is a receptor with only site b occupied. According to model 3,

$$P_o = \left(\frac{K_a K_b}{A^2\theta} + \frac{K_a + K_b}{A\theta} + \frac{1}{\theta} + 1\right)^{-1} \quad (3)$$

or

$$K_b = \frac{A^2\theta(P_o^{-1} - 1)}{A + K_a} - A \quad (4)$$

We define K_a to pertain to the α-δ site and assume that this value does not vary with the ϵ184 side chain. K_b values can be calculated for each patch from two experimental parameters, [ACh] and P_o, and two equilibrium constants, Θ (which is voltage dependent and is different for different ϵ184 mutants) and K_a.

K_b can also be estimated from the dose-response parameters. From model 3,

$$P_{o,max} = \frac{\theta}{1 + \theta} \quad (5)$$

$$EC_{50} = \frac{K_a + K_b + \sqrt{(K_a + K_b)^2 + 4K_aK_b(\theta + 1)}}{2(\theta + 1)}$$

Note that for wild-type AChRs, where the binding sites have equal affinities ($K_a = K_b$) and the gating process greatly favors opening ($\sqrt{\Theta} \gg 1$), Eq. 5 simplifies to

$$EC_{50} = \frac{K_d}{\sqrt{\theta}}. \quad (6)$$

Rearranging Eq. 5,

$$K_b = \frac{EC_{50}[EC_{50}(\theta + 1) - K_a]}{EC_{50} + K_a}. \quad (7)$$

Finally, we must correct the K_a and K_b estimates for each patch to account for competition between the agonist and extracellular K^+. Because the α-δ site is unaltered, we assume that the relationship between K_a and [KCl] is the same for all ϵ-subunit mutants:

$$K_a = \kappa_a\left(1 + \frac{[KCl]}{K_{I,a}}\right) \quad (8)$$

where $K_{I,a}$ is the equilibrium inhibition constant for K^+ (92 mM) and κ_a is the equilibrium dissociation constant for ACh in pure water at the α-δ site (70 μM; Akk and Auerbach, 1996). K_b, like K_a, will vary with the extracellular K^+, but $K_{I,b}$ and κ_b may differ for each ϵ-subunit mutation.

Mutations to ϵE184: ACh and K^+ affinity

Fig. 6 shows dose-response curves of AChRs with E, Q, D, and K side chains at ϵ184. Dose-response parameters for I and A mutants are given in Table 1. Compared to the wild type, the D, K, and I substitutions increase the EC_{50} and

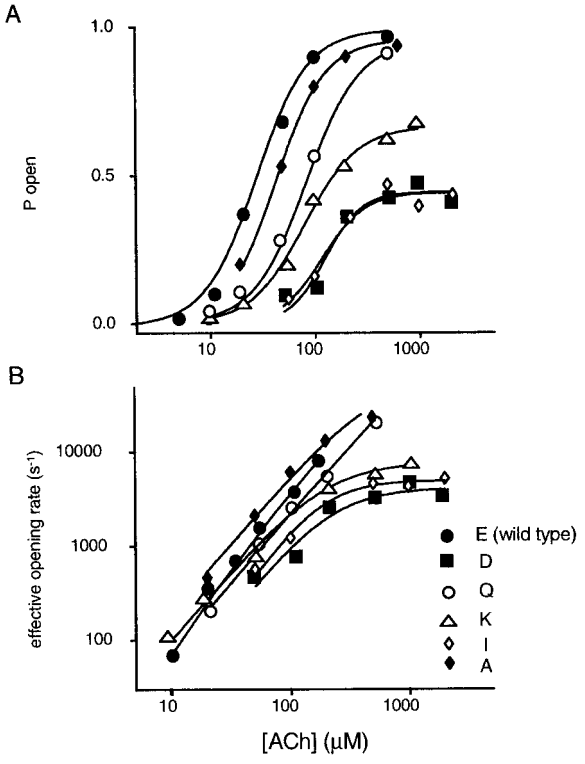

FIGURE 6 ϵE184 mutations and ACh affinity. (*A*) P_{open} versus [ACh]. All of the mutations increase the EC_{50}. The maximum P_{open} is significantly lower in the D, K, and I mutants. (*B*) The effective opening rate versus [ACh]. The maximum effective opening rate is lower in the K, D, and I mutants. The solid lines are fits by the Hill equation (Table 1). Each symbol is one patch.

lower the maximum of the P_o curve. The effect of varying the extracellular [KCl] on the ACh association rate constant (estimated by single-channel modeling) is shown in Fig. 7.

To determine the consequence of the mutation on both ACh and K^+ affinity, specifically at the α-ϵ site, for each patch K_b values were computed by combining Eqs. 4 and 8. The results are plotted as a function of the extracellular [KCl] in Fig. 8. These values were fitted by

$$K_b = \kappa_b\left(1 + \frac{[KCl]}{K_{I,b}}\right) \quad (9)$$

The fitted values of $K_{I,b}$ and κ_b for different ϵ184 side chains are given in Table 3.

First, we consider the $K_{I,b}$ values, which reflect the effect of the mutations on the affinity for K^+. Substitution of a positively charged lysine changed the net charge on the residue by +2 and essentially eliminated the competition by K^+. Substitution of a neutral glutamine changed the net charge by +1 and reduced the affinity of the receptor for K^+ by about fivefold. Substitution of a negatively charged aspartate did not change the net charge and did not change the affinity of the receptor for K^+. This is a logical progression that suggests that the ϵ184 side chain interacts electrostatically with K^+ at a site that competes with ACh. From the ϵE184Q mutation we estimate that the strength of this interaction is $\sim 1.7 k_B T/e$.

We next consider the κ_b values, which reflect the effect of the mutation on the intrinsic affinity (i.e., in the absence of K^+ competition) of the α-ϵ binding site for ACh. Recall that in wild-type AChR, ϵE184 is a negatively charged glutamate and $\kappa_b \approx 70\ \mu$M. κ_b values were not measured for

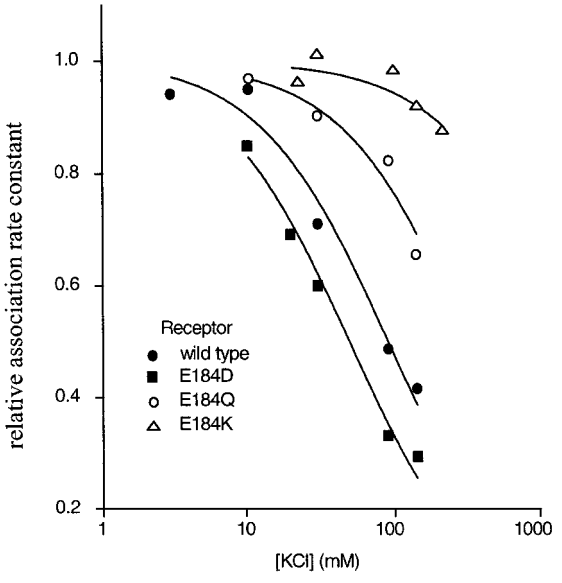

FIGURE 7 ϵE184 mutations and K^+ affinity. Increasing the extracellular [KCl] slows the apparent ACh association rate constant, estimated by single-channel modeling, assuming equivalent binding sites. The K^+ concentration that slows association by twofold is the equilibrium inhibition constant (K_I) for K^+ (see Table 3). Substitution of a positively charged lysine greatly lowers the affinity of the receptor for K^+.

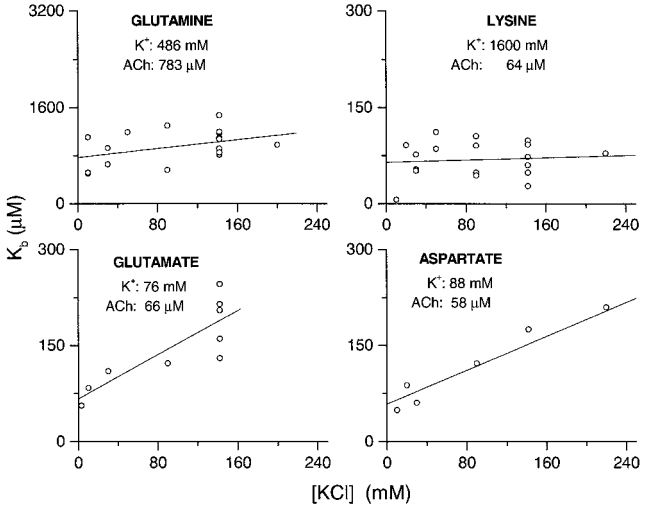

FIGURE 8 Effect of the ϵ184 side chain on ACh and K^+ affinities at the α-ϵ binding site. The equilibrium dissociation constant for ACh at the α-ϵ site (K_b) is plotted versus the extracellular concentration of KCl. The values are the equilibrium inhibition constant for K^+ and the equilibrium dissociation constant for ACh in pure water obtained from fitting by Eq. 9 (*solid line*; see Table 3). The affinity for K^+ was roughly equivalent with the acidic D and E side chains, about five times lower with the neutral Q side chain, and nearly 20 times lower with the positive K side chain. This pattern is consistent with a direct electrostatic interaction between ϵE184 and K^+. The affinity for ACh was similar for the E, D, and K side chains, but was more than 10 times lower for the Q side chain. This pattern suggests that the equilibrium dissociation constant for ACh is not determined by an electrostatic interaction with ϵE184.

ϵE184I and ϵE184A mutants. To estimate the intrinsic affinity (in pure water) of these mutants for ACh, we assumed that the $K_{I,b}$ value was the same as in ϵE184Q. The results are given in Table 3. Replacement of the negatively charged E with a neutral Q or A increased the equilibrium dissociation constant by more than 10-fold. However, replacement with either a negatively charged D, a positively charged K, or a neutral I had essentially no effect on the affinity of the receptor for ACh. This pattern of effects is not consistent with a simple electrostatic interaction between the ϵ184 side chain and ACh.

The effects of these mutations on gating are shown in Table 1. The channel opening rate constant was essentially unaltered by the Q and A substitutions, but was significantly reduced by K, D, and I mutations.

DISCUSSION

Mutations of putative binding site residues

We have examined mutations of four putative AChR binding site residues (αY93, αY198, ϵD175, and ϵE184). Previous studies had shown that mutation of these residues (or their homologs) resulted in an increase in the EC_{50} of normalized dose-response or binding curves. Here we have attempted to account for the observed changes in the dose-response curves in terms of more mechanistic properties of

the AChR, i.e., the equilibrium and/or rate constants for ACh binding, channel gating, and competitive inhibition by extracellular K^+.

ϵE184Q specifically lowered the affinity for ACh without changing the channel gating reaction. Because this mutation was not in the α-subunit, only one of the two binding sites was affected, presumably the one formed by the α- and ϵ-subunits. The ~10-fold decrease in affinity (in pure water) caused by this mutation translates to a destabilization of bound ACh by $\sim 2.3 k_B T$. This mutation similarly decreased the affinity of the receptor for extracellular K^+ by about fivefold ($1.7 k_B T$). ϵE184 remains a candidate residue for interacting directly with AChR ligands.

ϵD175N disrupted channel gating, mainly by lowering the channel opening rate constant. The affinities of both binding sites were unchanged by this mutation, and the 10-fold increase in the EC_{50} of the dose-response curve was completely accounted for by the nearly 80-fold decrease in the gating equilibrium constant. These results argue against the proposal that ϵD175 interacts directly with the quaternary amine moeity of ACh or with bound K^+. It is likely that the increase in the EC_{50} of the normalized binding curve consequent to mutation of the homologous residue in the γ-subunit (Czajkowski et al., 1993) is also attributable to an effect on gating, rather than binding.

αY93W and ϵD175N, and to a lesser extent αY198F, slowed both ACh association and dissociation, i.e., they decreased the ability of the agonist to move readily between the bulk solution and the transmitter docking site. In ϵD175N and αY198F the effect on association and dissociation was nearly symmetrical, so that the K_D for ACh was essentially unaltered. In αY93W there was a significant net destabilization of the bound transmitter molecule ($2.2 k_B T$). All of the mutations had little effect on the channel closing rate constant, and αY93W and ϵD175N, and to a lesser extent αY198F, slowed the opening rate constant.

This constellation of effects—reducing the ACh association and dissociation rate constants, slowing channel opening, and hardly influencing channel closing—is shared by two other binding site mutations, αD200N (Akk et al., 1996) and αY190F (Chen et al., 1995). This pattern is not what would be expected from specifically disrupting a favorable interaction between the mutated residues and the bound ACh molecule, where the mutation might be expected to increase k_- and K_D, and to perhaps have relatively little effect on β. Rather, the results suggest that the mutations (in particular, αY93W) cause a more delocalized change in the structure of the binding pocket that compromises both the mobility of the ligand into and out of its docking site and the high speed of channel opening.

The mutations αY93W and αY198F also had no measurable effect on competition by extracellular K^+, which suggests that these residues probably do not contribute to the cation-binding site(s) or to other structures that influence the access of K^+ to this site.

Mutations of ϵE184

Six side chains of ϵ184 were examined: E, Q, D, K, I, and A. Receptors with a K, E, D, or I side chain had approximately the same intrinsic affinity for ACh (i.e., in pure water; Table 3), whereas substitution of a Q or an A increased the ACh equilibrium dissociation constant by about 10-fold. The basis for this change in affinity is unclear, but the fact that AChRs with a positive, negative, or neutral side chain at ϵE184 have the same affinity for ACh strongly argues against an electrostatic interaction between the ϵ184 side chain and ACh. With regard to channel gating, the opening rate constant remained fast with E, Q, and A side chains, but was significantly slowed upon substitution of a K, D, or I. Of the residues we examined, only E supported both a high affinity for ACh and efficient gating.

Mutations to ϵ184 had substantial effects on competitive inhibition by extracellular cations (Fig. 8; Table 3). The affinity for K^+ decreased ~20-fold when the side chain was positive (K) and decreased by about fivefold when the side chain was neutral (Q) compared to when it was negative (E and D). The E-to-Q mutation also reduced the ionic selectivity of the competition between Na^+, K^+, and Cs^+. These results suggests that the ϵE184 side chain determines, in part, inorganic cation affinity and selectivity via a direct electrostatic interaction. From the magnitude of the effects we estimate that loss of a negative charge at residue ϵ184 destabilizes K^+ by $\sim 1.7 k_B T$.

We can estimate the product of the charge separation distance (d) and the dielectic constant (ϵ) from Coulomb's law (Hille, 1992):

$$\Delta G_{K_I} \text{ (in } k_B T) = 545 \Delta z / \epsilon d \text{ (in Å)} \qquad (10)$$

where Δz is the net change in the charge of residue ϵE184. From the E-to-Q mutation we estimate that $\epsilon d = 320$ Å. If the dielectric at the surface of a protein is ~40 (Laberge, 1998), then we estimate that the separation between the carbonyl of ϵE184 and K^+ is ~8 Å. This distance is in rough accord with the observation that in barnase there is an electrostatic interaction of $\sim 0.7 k_B T$ between surface residues separated by 12 Å (Loewenthal et al., 1993).

Physical models of binding

In this section we discuss physical models for equilibrium binding of ACh^+ and K^+ to the α-ϵ site. Our goal is to account for the observation that K^+ binding is influenced by an electrostatic interaction with ϵE184, whereas ACh^+ binding is not.

We can reject the simplest model of binding, where both ligands directly compete for a single spot. In such a static, single-site mechanism, the K_D for ACh^+ and the K_I for K^+ are each simply the ratio of the dissociation and association rate constants for each ligand. Given an electrostatic interaction with both cationic ligands, we would expect that changing the charge of the ϵ184 side chain would alter both equilibrium constants. Whereas this was the case with the Q

mutation, the K and D mutations only changed the affinity for K^+. This simple physical model of binding does not account for the results.

The second physical model we consider is motivated by the structure of acetylcholinesterase, which shows that the substrate must traverse a distributed binding domain (a "gorge") on its path from the bulk solution to its docking site (Sussman et al., 1991; Radic et al., 1997). In addition, in this enzyme occupancy of a peripheral anionic site impedes substrate binding to the active center (Radic et al., 1994). With regard to AChR, in this model we propose that at each transmitter binding site there are multiple ligand binding sites in series. Minimally, there would be an outer site and a docking site. We assume that the trajectory of a ligand from the bulk solution to the docking site requires single filing. Thus ACh^+ and K^+ compete even if K^+ cannot penetrate to the docking site. In this model the outer and docking sites could be physically separated.

If the occupancy of the outer site by ACh^+ is brief, the apparent rates for the agonist moving between the bulk solution and the docking site (k_+ and k_-) and the apparent equilibrium dissociation constant for an agonist (K_D) are

$$k_+ = k_{01}\left(1 + \frac{k_{10}}{k_{12}}\right)^{-1}$$

$$k_- = k_{21}\left(1 + \frac{k_{12}}{k_{10}}\right)^{-1} \qquad (11)$$

$$K_b = \frac{k_{01}k_{10}}{k_{12}k_{21}}$$

where k_{01} is the rate constant for moving from the external solution to the outer site, k_{10} is the rate constant for returning to the solution from the outer site, k_{12} is the rate constant for moving from the outer site to the docking site, and k_{21} is the rate constant for moving from the docking site to the outer site.

If the ϵ184 side chain interacts electrostatically only with the ligand that resides in the outer site, changing the charge of this side chain will change the relative magnitude of k_{10} and k_{12}. Thus for competitive inhibitors (like K^+) that occupy only the outer site, $K_I = k_{01}/k_{10}$, and changing the charge on ϵ184 will change affinity in a predictable way, increasing as the side chain becomes more positive. For agonists (like ACh^+) that reach the docking site, K_D is a function of the ratio of the altered rate constants, and the effects of changing the charge cancel. Therefore, according to the static, multisite model, changing the charge in ϵ184 will have no effect on the apparent equilibrium dissociation constant for ACh^+. This model accounts for the observation that E, Q, and K side chains have logical effects on K_I in terms of electrostatics but more erratic effects on the K_D for ACh.

A third physical model for ACh^+ and K^+ binding sites is derived from the "induced-fit" model of enzymes (Koshland, 1970; Bennett and Steitz, 1980; Fersht et al., 1988). In this scheme there is only one site for which both ligands compete. A conformational change induced by the presence of an agonist switches this site between a resting, ultralow affinity conformation ($K_D > 1000\ \mu M$) to one with a higher affinity for agonists ($K_D \approx 100\ \mu M$ for ACh^+). Note that this conformational change is distinct from, but perhaps related to, the conformational change that constitutes channel gating, and that this higher affinity form is distinct from the one that accompanies channel opening and desensitization, where $K_D \approx 0.05\ \mu M$ for ACh^+ (Sine et al., 1995; see Auerbach and Akk, 1998). When the binding site is in the ultralow affinity form, the dissociation rate constant of either K^+ and ACh^+ is fast and the ligand can freely exchange with the bulk solution. The ligand only becomes "bound" when the site assumes its higher affinity conformation. ACh^+ has bonds that rotate freely; thus the agonist, too, may change its conformation as part of the "induced fit".

In this model, we propose that K^+ can occupy the site but cannot induce the conformational switch. Thus electrostatic interactions between the ϵ184 side chain and the site are indeed manifest as a logical change in the K_I for K^+. However, for agonists (i.e., ligands that induce the conformation change), the kinetic and equilibrium equations for this induced-fit model are identical to those for the two-site model (Eq. 11), assuming that the conformational switching rates are rapid and with the following changes in definition: k_{12} is the rate constant for changing from the lower to higher form, and k_{21} is the rate constant for the reverse process. That is, if the charge on ϵ184 influences only binding and not the conformational switch, then we would detect the electrostatic effect on the selectivity and equilibrium constant for ionic competition, but not on the K_D for the agonist.

Another physical model that combines features of the two-site and induced-fit schemes is the "conformational gating" mechanism that has been proposed for substrate binding to acetylcholinesterase (Zhou et al., 1998). In this mechanism, to bind to the catalytic site the substrate must first pass a barrier that rapidly fluctuates between open and closed positions. This scheme, like the two-site and induced-fit models, can be described by a two-barrier, one-well energy model and can therefore account (via Eq. 11) for the observation that the charge on the ϵE184 side chain differentially effects K^+ and ACh^+ equilibrium binding.

Our results do not allow us to distinguish between the static, two-site, and induced-fit mechanisms for binding. There is precedent for both models, and binding may involve both passage through a distributed pathway as well as conformational adjustments. However, certain considerations lead us to favor the induced-fit hypothesis. First, if outer and docking sites can be occupied simultaneously, the multisite model predicts that the dissociation rate constant for ACh^+ will be slowed by external K^+. The evidence indicates that this rate constant is independent of the external K^+ concentration (Akk and Auerbach, 1996). Second, in the multisite model the protein is static, whereas in the

induced-fit model there is a conformational change at each binding site consequent to ligand-protein contact. Such a conformational event has previously been proposed to account for the different voltage dependences of un-, mono-, and diliganded AChR (Auerbach et al., 1996; see also Auerbach, 1993). Third, the induced-fit model offers a mechanism to account for the correlation between the agonist association rate constant and the rate constant for channel opening for different agonists (Zhang et al., 1995) and mutants. The conformational change that is the "induced fit" may be graded and agonist dependent and may also have the consequence of changing the nature of the transition state that separates open and closed channel structures. Thus a weaker agonist (e.g., TMA^+) might contribute less binding energy, leading not only to a higher K_D but also to a slower channel opening rate constant. The induced-fit model offers an explanation for why affinity and efficacy are correlated (Post and Ray, 1995).

SUMMARY

Despite the difficulty of making inferences about structure from purely functional results, our experiments offer the following general insights. Normalized dose-response and binding curves are "macroscopic" in nature, and changes in agonist binding, channel gating, and ion competition combine to determine the shape and position of these profiles. A mutation-induced change in the EC_{50} is not sufficient evidence to conclude that there is a direct interaction between the mutated residue and the agonist molecule. The parameter that provides the clearest measure of the effect of a mutation on agonist affinity per se is the equilibrium dissociation constant extrapolated to its value in pure water. When the AChR is in its closed channel conformation, the transmitter binding site is a delicate structure that is readily disturbed by a variety of perturbations, including mutations to residues that may be located at some distance from the agonist docking site. Finally, we propose that binding is a complex process that could involve multiple sites of interaction and/or conformational changes in both the ligand and the protein.

We thank Steven Sine for kindly providing the αY93W and αY198F mutants, Arthur Karlin and Claudio Grosman for comments on the manuscript, and Karen Lau for technical assistance.

This work was supported by NS-23513.

REFERENCES

Abramson, S. N., Y. Li, P. Culver, and P. Taylor. 1989. An analog of lophotoxin reacts covalently with Tyr^{190} in the α-subunit of the nicotinic acetylcholine receptor. *J. Biol. Chem.* 264:12666–12672.

Akk, G., and A. Auerbach. 1996. Inorganic, monovalent cations compete with agonists for the transmitter binding site of nicotinic acetylcholine receptors. *Biophys. J.* 70:2652–2658.

Akk, G., S. Sine, and A. Auerbach. 1996. Binding sites contribute unequally to the gating of mouse nicotinic αD200N acetylcholine receptors. *J. Physiol. (Lond.).* 496:185–196.

Auerbach, A. 1993. A statistical analysis of acetylcholine receptor activation in *Xenopus* myocytes: stepwise vs. concerted models of gating. *J. Physiol. (Lond.).* 461:339–378.

Auerbach, A., and G. Akk. 1998. Desensitization of mouse nicotinic acetylcholine receptor channels: a two-gate mechanism. *J. Gen. Physiol.* 112:181–197.

Auerbach, A., W. Sigurdson, J. Chen, and G. Akk. 1996. Different gating charge movements in doubly-, singly-, and unliganded acetylcholine receptors. *J. Physiol. (Lond.).* 494:155–170.

Ausubel, F. M., R. Brent, R. E. Kingston, D. D. Moore, J. G. Seidman, J. A. Smith, and K. Struhl. 1992. Short Protocols in Molecular Biology. John Wiley and Sons, New York.

Bennett, W. S., Jr., and T. A. Steitz. 1980. Structure of a complex between yeast hexokinase A and glucose. *J. Mol. Biol.* 140:211–230.

Blount, P., and J. P. Merlie. 1989. Molecular basis of the two nonequivalent ligand binding sites of the muscle nicotinic acetylcholine receptor. *Neuron.* 3:349–357.

Charnet, P., C. Labarca, and H. A. Lester. 1992. Structure of the gammaless nicotinic acetylcholine receptor: learning from omission. *Mol. Pharmacol.* 41:708–717.

Chen, J., Y. Zhang, G. Akk, S. Sine, and A. Auerbach. 1995. Activation kinetics of recombinant mouse nicotinic acetylcholine receptors: mutations of α-subunit tyrosine 190 affect both binding and gating. *Biophys. J.* 69:849–859.

Czajkowski, C., and A. Karlin. 1991. Agonist binding site of *Torpedo* electric tissue nicotinic acetylcholine receptor. *J. Biol. Chem.* 266: 22603–22612.

Czajkowski, C., C. Kaufmann, and A. Karlin. 1993. Negatively charged amino acid residues in the nicotinic receptor delta subunit that contribute to the binding of acetylcholine. *Proc. Natl. Acad. Sci. USA.* 90: 6285–6289.

Dennis, M., J. Giraudat, F. Kotzyba-Hibert, M. Goeldner, C. Hirth, J. Y. Chang, C. Lazure, M. Chretien, and J. P. Changeux. 1988. Amino acids of the *Torpedo marmorata* acetylcholine receptor a subunit labeled by a photoaffinity ligand for the acetylcholine binding site. *Biochemistry.* 27:2346–2357.

Devillers-Thiery, A., J. L. Galzi, J. L. Eisele, S. Bertrand, D. Bertrand, and J. P. Changeux. 1993. Functional architecture of the nicotinic acetylcholine receptor: a prototype of ligand-gated ion channels. *J. Membr. Biol.* 136:97–112.

Fersht, A. R., J. W. Knill-Jones, H. Bedouelle, and G. Winter. 1988. Reconstruction by site-directed mutagenesis of the transition state for the activation of tyrosine by the tyrosyl-tRNA synthetase: a mobile loop envelopes the transition state in an induced-fit mechanism. *Biochemistry.* 27:1581–1587.

Filatov, G. N., and M. M. White. 1995. The role of conserved leucines in the M2 domain of the acetylcholine receptor in channel gating. *Mol. Pharmacol.* 48:379–384.

Galzi, J. L., F. Revah, D. Black, M. Goeldner, C. Hirth, and J. P. Changeux. 1990. Identification of a novel amino acid a-tyrosine 93 within the cholinergic ligands-binding sites of the acetylcholine receptor by photoaffinity labeling. *J. Biol. Chem.* 265:10430–10437.

Hamill, O. P., A. Marty, E. Neher, B. Sakmann, and F. J. Sigworth. 1981. Improved patch-clamp techniques for high-resolution current recording from cells and cell-free membrane patches. *Pflugers Arch.* 391:85–100.

Higuchi, R. 1990. Recombinant PCR. *In* PCR Protocols. A Guide to Methods and Applications. M. A. Innis, D. H. Gelfand, J. J. Sninsky, and T. J. White, editors. Academic Press, San Diego, CA. 177–183.

Hille, B. 1992. Ionic Channels of Excitable Membranes. Sinauer Associates, Sunderland, MA.

Jones, M. V., Y. Sahara, J. A. Dzubay, and G. Westbrook. 1998. Defining affinity with the $GABA_A$ receptor. *J. Neurosci.* 18:8590–8604.

Karlin, A., and M. H. Akabas. 1995. Toward a structural basis for the function of nicotinic acetylcholine receptors and their cousins. *Neuron.* 15:1231–1244.

Koshland, D. E., Jr. 1970. The molecular basis for enzyme regulation. *In* The Enzymes. Paul D. Boyer, editor. Academic Press, New York.

Labarca, C., M. W. Nowak, H. Zhang, L. Tang, P. Deshpande, and H. A. Lester. 1995. Channel gating governed symmetrically by conserved leucine residues in the M2 domain of nicotinic receptors. *Nature.* 376: 514–516.

Laberge, M. 1998. Intrinsic protein fields: basic non-covalent interactions and relationship to protein-induced Stark effects. *Biochim. Biophys. Acta.* 1386:305–330.

Lowenthal, R., J. Sancho, T. Reinikainen, and A. Fersht. 1993. Long-range charge–charge interactions in proteins. *J. Mol. Biol.* 232:574–583.

Martin, M., C. Czajkowski, and A. Karlin. 1996. The contributions of aspartyl residues in the acetylcholine receptor gamma and delta subunits to the binding of agonists and competitive antagonists. *J. Biol. Chem.* 271:13497–13503.

Middleton, R. E., and J. B. Cohen. 1991. Mapping of the acetylcholine binding site of the nicotinic acetylcholine receptor: [^{3}H]nicotine as an agonist photoaffinity label. *Biochemistry.* 30:6987–6997.

Nowak, M. W., P. C. Kearney, J. R. Sampson, M. E. Saks, C. G. Labarca, S. K. Silverman, W. Zhong, J. Thorson, J. N. Abelson, N. Davidson, P. G. Schultz, D. A. Dougherty, and H. A. Lester. 1995. Nicotinic receptor binding site probed with unnatural amino acid incorporation in intact cells. *Science.* 268:439–442.

O'Leary, M. E., and M. M. White. 1992. Mutational analysis of ligand-induced activation of the *Torpedo* acetylcholine receptor. *J. Biol. Chem.* 267:8360–8365.

Pedersen, S. E., and J. B. Cohen. 1990. *d*-Tubocurarine binding sites are located at α-γ and α-δ subunit interfaces of the nicotinic acetylcholine receptor. *Proc. Natl. Acad. Sci. USA.* 87:2785–2789.

Post, C. B., and W. J. Ray, Jr. 1995. Reexamination of induced fit as a determinant of substrate specificity in enzymatic reactions. *Biochemistry.* 34:15881–15885.

Prince, R. J., and S. M. Sine. 1996. Molecular dissection of subunit interfaces in the acetylcholine receptor. Identification of residues that determine agonist selectivity. *J. Biol. Chem.* 271:25770–25777.

Qin, F., A. Auerbach, and F. Sachs. 1996. Estimating single-channel kinetic parameters from idealized patch-clamp data containing missed events. *Biophys. J.* 70:264–280.

Qin, F., A. Auerbach, and F. Sachs. 1996a. Idealization of single-channel currents using the segmental k-means method. *Biophys. J.* 70:A227.

Radic, Z., R. Duran, D. C. Vellom, Y. Li, C. Cervenansky, and P. Taylor. 1994. Site of fasciculin interaction with acetylcholinesterase. *J. Biol. Chem.* 269:11233–11239.

Radic, Z., P. D. Kirchhoff, D. M. Quinn, J. A. McCammon, and P. Taylor. 1997. Electrostatic influence on the kinetics of ligand binding to acetylcholinesterase. *J. Biol. Chem.* 272:23265–23277.

Sachs, F. 1983. Automated analysis of single-channel records. *In* Single-Channel Recording. B. Sakmann and E. Neher, editors. Plenum Press, New York. 265–286.

Sakmann, B., J. Patlak, and E. Neher. 1980. Single acetylcholine-activated channels show burst-kinetics in presence of desensitizing concentrations of agonist. *Nature.* 286:71–73.

Sine, S. M. 1993. Molecular dissection of subunit interfaces in the acetylcholine receptor: identification of residues that determine curare selectivity. *Proc. Natl. Acad. Sci. USA.* 90:9436–9440.

Sine, S. M., and T. Claudio. 1991. Gamma- and delta-subunits regulate the affinity and the cooperativity of ligand binding to the acetylcholine receptor. *J. Biol. Chem.* 266:19369–19377.

Sine, S. M., K. Ohno, C. Bouzat, A. Auerbach, M. Milone, J. N. Pruitt, and A. G. Engel. 1995. Mutation of the acetylcholine receptor α subunit causes a slow-channel myasthenic syndrome by enhancing agonist binding activity. *Neuron.* 15:229–239.

Sine, S. M., P. Quiram, F. Papanikolaou, H. J. Kreienkamp, and P. Taylor. 1994. Conserved tyrosines in the alpha subunit of the nicotinic acetylcholine receptor stabilize quaternary ammonium groups of agonists and curariform antagonists. *J. Biol. Chem.* 269:8808–8816.

Sine, S. M., and P. Taylor. 1980. The relationship between agonist occupation and the permeability response of the cholinergic receptor revealed by bound cobra alpha-toxin. *J. Biol. Chem.* 255:10144–10156.

Sussman, J. L., M. Harel, F. Frolow, C. Oefner, A. Goldman, L. Toker, and I. Silman. 1991. Atomic structure of acetylcholinesterase from *Torpedo californica:* a prototype acetylcholine-binding protein. *Science.* 253: 872–879.

Tomaselli, G. F., J. T. McLaughlin, M. E. Jurman, E. Hawrot, and G. Yellen. 1991. Mutations affecting agonist sensitivity of the nicotinic acetylcholine receptor. *Biophys. J.* 60:721–727.

Tsigelny, I., N. Sugiyama, S. M. Sine, and P. Taylor. 1997. A model of the nicotinic receptor extracellular domain based on sequence identity and residue location. *Biophys. J.* 73:52–66.

Unwin, N. 1993. Nicotinic acetylcholine receptor at 9 Å resolution. *J. Mol. Biol.* 229:1101–1124.

Unwin, N. 1995. Acetylcholine receptor channel imaged in the open state. *Nature.* 373:37–43.

Unwin, N. 1996. Projection structure of the nicotinic acetylcholine receptor: distinct conformations of the alpha subunits. *J. Mol. Biol.* 257:586–596.

Valenzuela, C. F., E. P. Weign, J. Yguerabide, and D. A. Johnson. 1994. Transverse distance between the membrane and agonist binding sites on the *Torpedo* acetyl-choline receptor: a fluorescence study. *Biophys. J.* 66:674–682.

Wang, H. L., A. Auerbach, N. Bren, K. Ohno, A. G. Engel, and S. M. Sine. 1997. Mutation in the M1 domain of the acetylcholine receptor alpha subunit decreases the rate of agonist dissociation. *J. Gen. Physiol.* 109:757–766.

Zhang, Y., J. Chen, and A. Auerbach. 1995. Activation of recombinant mouse acetylcholine receptors by acetylcholine, carbamylcholine and tetramethylammonium. *J. Physiol. (Lond.).* 486:189–206.

Zhou, H., S. Wlodek, and J. A. McCammon. 1998. Conformational gating as a mechanism for enzyme specificity. *Proc. Natl. Acad. Sci. USA.* 95:9280–9283.